

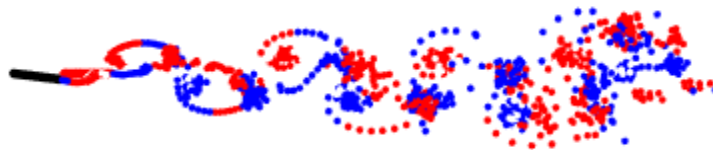
# Unsteady Flow Past Tandem Flat Plates

(Project Report)

AS5470

Alan John Varghese - AE16B019

Achu Shankar - AE16B102



# 1 Introduction

The unsteady behaviour of systems is of crucial importance in turbines, rotorcrafts, tandem wing planes and so on. More recently, studies on unsteady aerodynamics of airfoils have been motivated by the prospect of utilizing the advantages of large unsteady aerodynamic forces for aerospace applications like increased maneuverability of fighter aircraft, use of micro-UAVs, which are designed for very small payloads for remote-sensing operations in areas of limited access and the use of multi-UAVs in formation for surveillance purposes to increase their longevity and endurance.

In this project we analyze the unsteady flow past two flat plates separated by a distance, typically referred to as the tandem wing configuration. Airplanes with tandem wings were manufactured in the early 1940s on an experimental basis. They are unpopular now since it was not seen to have a significant advantage compared to the conventional airplanes. Recently, Dr Yoshinobu Inada [1] from Tokai University, Japan studied a species of fish called 'ribbon halfbeak' with the ability to fly, despite lacking the necessary hind wing fins. In their study, they attribute the capability of flight in 'ribbon halfbeak', to its tandem wing configuration. Studies like these could give insightful information to aid optimal design of tandem wing aircrafts.

We develop a lumped vortex method to simulate the flow past a tandem wing. High fidelity CFD solvers have proven to be great tools in calculating loads and the flow field around the system. But high fidelity CFD solvers are computationally expensive. Potential flow methods like lumped vortex methods which we implement here, have significance in this context as they take much less time compared to CFD solvers. Even though the accuracy of the solution obtained is not at par with CFD solvers, it is sufficient for a lot of engineering applications.

## 2 Unsteady Lumped Vortex Solver

Lumped vortex method was used due to its simplicity and computational efficiency. Here, the flat plate is discretised into panels consisting of a point vortex and a collocation point, where the no normal flow is enforced[2][3]. Wakes are released along the flat plate at a distance of  $\epsilon U_\infty \Delta t$ . The wake strength of the new wake can be calculated using Kelvins condition. Enforcing these conditions gives rise to a linear system of equations as shown in Equation (1).  $\Gamma_A$  and  $\Gamma_B$  represents the strength of the body bound vortices of plate A and B respectively.  $\Gamma_{WA}$  and  $\Gamma_{WB}$  represents the strength of the latest shed vortex from plate A and B respectively. F1 represents the influence of the body bound vortices of plate A at collocation points of A itself and F2 represents the influence of the body bound vortices of B at collocation points of A. Similarly G1 and G2 represent the influence of body bound vortices of plate A and B respectively at the collocation points of plate B. F3, F4, G3 and G4 represents the effect due to the last shed wake from each plate on each other and to itself. L1 is a  $(1*N)$  vector of ones, L2 is a  $(1*N)$  vector of zeroes, L3 is 1 and L4 is 0. Similarly, M1 is a  $(1*N)$  vector of zeros, M2 is a  $(1*N)$  vector of zeroes, M3 is 0 and M4 is 0.  $rhs_A$  and  $rhs_B$  is the no normal condition on plate A and B respectively.

$$\begin{pmatrix} F1 & F2 & F3 & F4 \\ G1 & G2 & G3 & G4 \\ L1 & L2 & L3 & L4 \\ M1 & M2 & M3 & M4 \end{pmatrix} \begin{pmatrix} \Gamma_A \\ \Gamma_B \\ \Gamma_{WA} \\ \Gamma_{WB} \end{pmatrix} = \begin{pmatrix} rhs_A \\ rhs_B \\ \sum \Gamma(t - \Delta t)_A \\ \sum \Gamma(t - \Delta t)_B \end{pmatrix} \quad (1)$$

$$AX = B \quad (2)$$

$$\begin{aligned}
F1 &= ( )_{N \times N}, & F2 &= ( )_{N \times N}, & G1 &= ( )_{N \times N}, & G2 &= ( )_{N \times N} \\
F3 &= ( )_{N \times 1}, & F4 &= ( )_{N \times 1}, & G3 &= ( )_{N \times 1}, & G4 &= ( )_{N \times 1} \\
L1 &= (1..1)_{1 \times N}, & L2 &= (0..0)_{1 \times N}, & M1 &= (0..0)_{1 \times N}, & M2 &= (1..1)_{1 \times N} \\
L3 &= 1, & L4 &= 0, & M3 &= 0, & M4 &= 1 \\
\Gamma_A &= ( )_{N \times 1}, & \Gamma_B &= ( )_{N \times 1}, & \Gamma_{WA} &= ( )_{1 \times 1}, & \Gamma_{WB} &= ( )_{1 \times 1}
\end{aligned}$$

Solving the linear system gives the strength of the bound vortexes and the wake of both the plates at each time step. The generated wakes are free to move in space and are influenced by all the vortexes present as well as the free stream velocity, a time-stepping method is used to update the location of the shed vortexes at the end of each time step.

### 3 Near field vortex-solid interaction

As the vortexes move freely the wake vortexes of the leading airfoil interact with the trailing airfoil before travelling with the free-stream. Computationally, this condition will lead to numerical singularities and physically, it is expected that a free vortex will dissipate when it hits a solid surface. To model the vortex surface interaction the method prescribed in the paper [4] is used. The vortexes that satisfy the condition 3 are artificially dissipated. Whenever a wake vortex satisfies this condition, its influence on the flow-field, i.e. the velocity induced by it on the bound vortexes, wake vortexes and hence, the wake shape is ignored since it is considered dissipated.

$$r \leq 0.01c \quad (3)$$

### 4 Unsteady lift calculation

The pressure difference between the airfoil's upper and lower surfaces of flat plate is obtained using the Bernoulli equation near the panel surface. The pressure difference at the  $j^{th}$  panel is obtained to be

$$\Delta p_j = \rho [(U + u_w, w_w)_j \cdot \tau_j \frac{\Gamma_j}{\Delta l_j} + \frac{\partial}{\partial t} \sum_{k=1}^j \Gamma_k]$$

Here,  $u_w$  and  $w_w$  are the velocity at the corresponding collocation point induced by wakes shed from both the flat plates.  $\tau_j$  is the tangent at the  $j - th$  collocation point and  $\Delta l_j$  is the width of each panel. And  $\sum_{k=1}^j \Gamma_k$  denotes the sum of the vortex strengths of each body bound vortex of that aerofoil until the  $j - th$  panel.

The total lift across a flat plate is obtained by summing over the lift of each panel, and is given by:

$$L = \sum_{j=1}^N \Delta p_j \Delta l_j \cos \alpha_j$$

## 5 Numerical results

### 5.1 Analysis of a single flat plate

#### 5.1.1 Transient motion to an AOA

Analysis of transient motion of flat plates to a certain AOA was done in order to check the accuracy of the solver. The airfoils were placed at large distance from each other ( $100c$ ), to minimise the effects each has on one another, essentially each plate behaves as a single plate undergoing transient pitch. Figure 1a shows the wake shape and figure 1a shows the value of  $c_l$  as a function of  $\tau$ . The values of  $c_l$  obtained

numerically was compared with values obtained using classical unsteady analysis using wagner function. It can be observed that both the values converge to same value as  $\tau$  increases. The initial overshoot in the numerical value maybe attributed to the loss in accuracy of the numerical approach. This trend was mentioned in 'Low-speed aerodynamics' [2] as well as in the research studies conducted by H. Aziz and R.Mukherjee [4]. The wakeshape is consistent with the starting vortex usually observed in such a system.

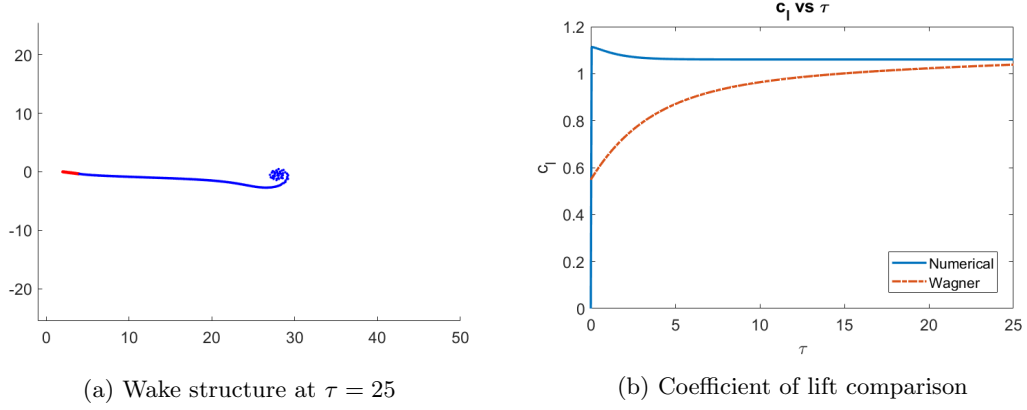


Figure 1

### 5.1.2 Pitching motion

Again the plates were placed at a large distance minimizing the effect on each other and the plates were given a pitching motion governed by equation 4. Analysis of the wake structure, figure 2a, shows the generation of reverse Karman wakes from the the trailing edge. This is in agreement with the real behaviour. The maximum lift coefficient obtained is 3.08, comparing with a quasi-steady analysis result, which gives a value of  $c_{l_{max}} = 3.28$ .

$$\alpha = \frac{10\pi}{180} \sin \omega t \quad (4)$$

The value of the parameters used

$$U_\infty = 5, \quad \kappa = \frac{\omega c}{2U_\infty} = 1 \quad \text{and} \quad \tau = \frac{tV_\infty}{c} = 25$$

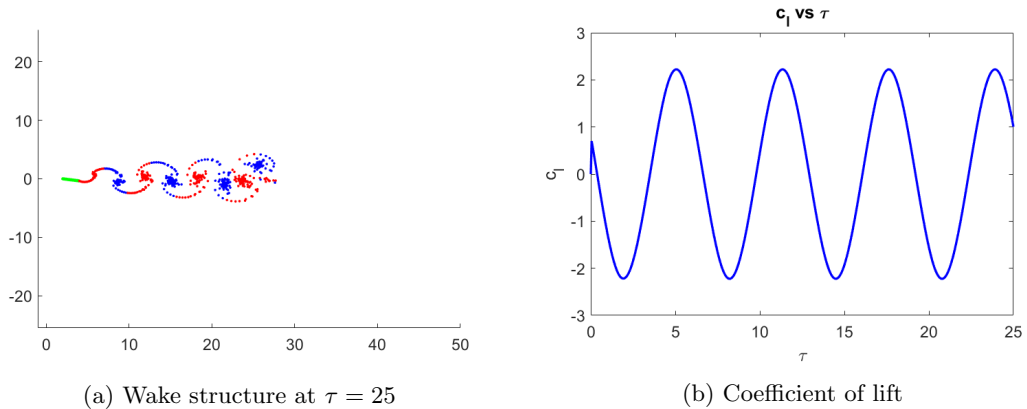


Figure 2

From the above two analysis the feasibility of using the developed lumped vortex solver for further analysis was verified.

## 5.2 Effect of separation between the flat plates

In this section the effect of separation distance ( $d$ ), defined as the distance between the trailing edge of plate 1 to leading edge of plate 2, on the loads experienced by the plates and the wake structure was analysed. In all the analysis discussed in this subsection  $U_\infty = 5m/s$ , and the kinematics of plate 1 is given by the expression,

$$\alpha = \frac{10\pi}{180} \cos \omega t \quad (5)$$

with  $\kappa = 1$  and plate 2 is stationary with an AOA of  $0^\circ$ . The figures below shows the wake structure and the coefficient of lift of both the plates.

**d = 0.1m**

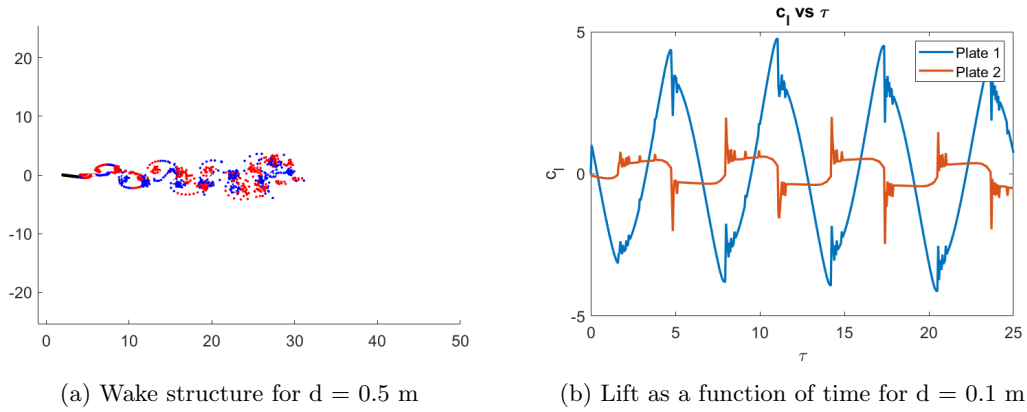


Figure 3

**d = 0.5m**

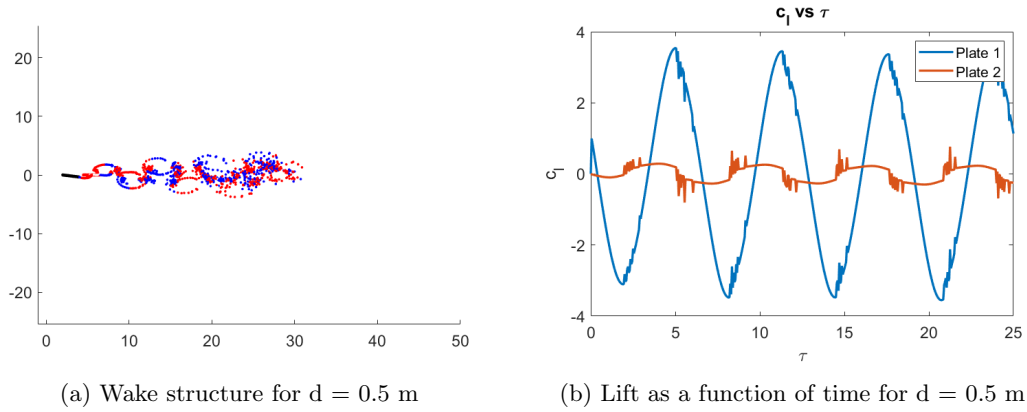
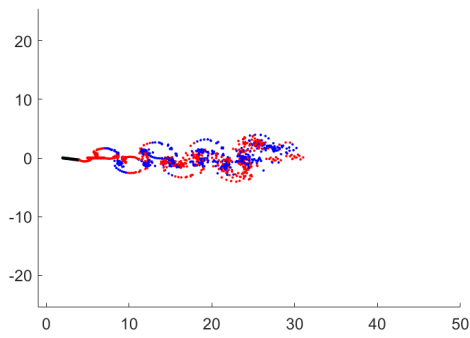
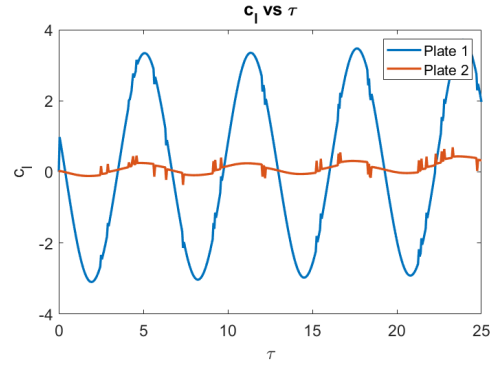


Figure 4

$d = 1 \text{ m}$



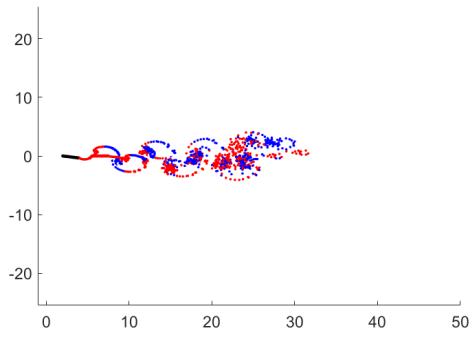
(a) Wake structure for  $d = 1 \text{ m}$



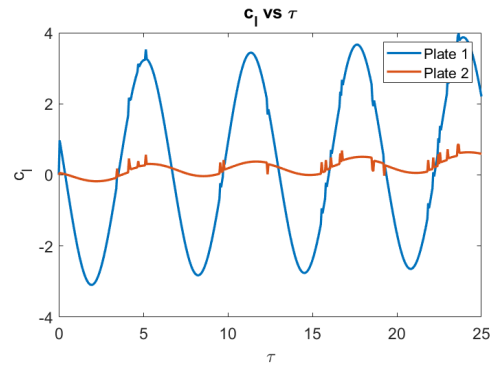
(b) Lift as a function of time for  $d=1\text{m}$

Figure 5

$d = 1.5 \text{ m}$



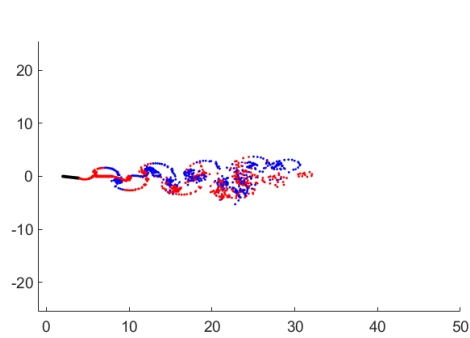
(a) Wake structure for  $d = 1.5 \text{ m}$



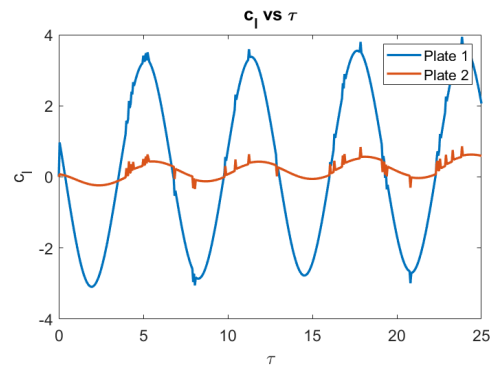
(b) Coefficient vs time for  $d=1.5\text{m}$

Figure 6

$d = 2 \text{ m}$



(a) Wake structure for  $d = 2 \text{ m}$



(b) Coefficient of lift vs time for  $d=2 \text{ m}$

Figure 7

$d = 5 \text{ m}$

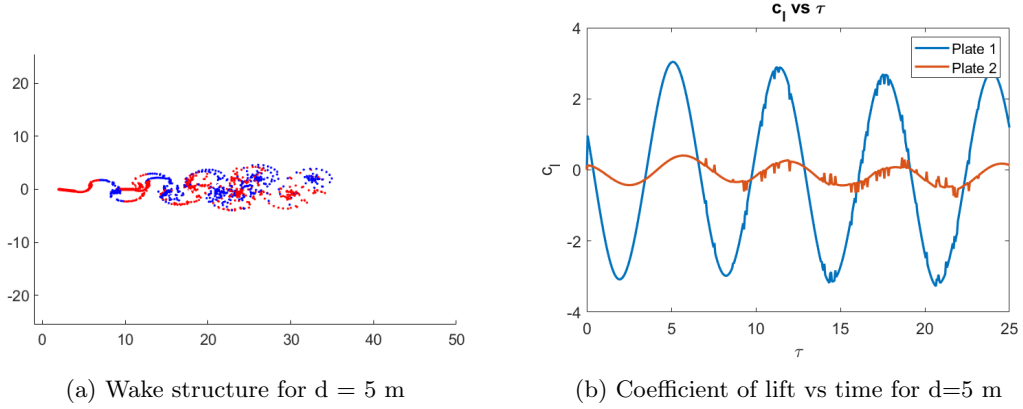


Figure 8

$d = 10 \text{ m}$

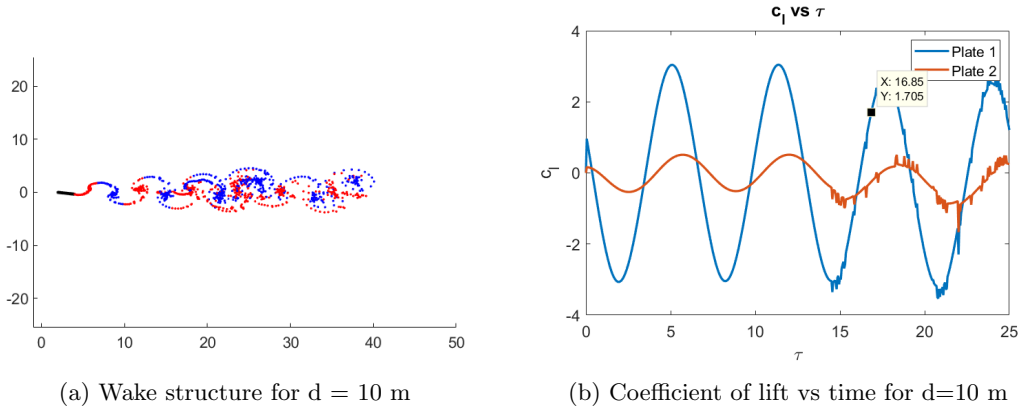


Figure 9

Analysing the above data some peculiar features arise,

1. Due to the periodic motion in plate 1 a periodic lift was generated in plate 2 as well. This is due to the fact that, the inflow plate 2 sees, is one which is greatly affected by kinematics and shed vortices of plate 1. Also the frequency of lift induced on plate 2 is same as pitching frequency of plate 1.
2. For all values of  $d$  it can be observed that there are some noises in the  $c_l$  data. The time when the data becomes noisy is roughly the same as the time at which the shed vortices from plate 1 reaches plate 2. Hence the time at which the noise onsets is a function of  $d$  (keeping  $U_\infty$  constant). The source of the noise is mostly due to interaction of the potential vortex on plate 2 and the abrupt removal of the vortex to model the dissipation of vortex due to vortex body interaction.
3. There is a time lag between the occurrence of maximum lift on plate 2 and plate 1. It decreases as  $d$  is increased from 0.1 to 1, in-between  $d=1$  and  $d=1.5$  it becomes zeros and after that it changes its sign. The time lag tends to a constant value with further increase in value of  $d$  Figure 10c summarises these observations.
4. Figure 10a shows the variation of  $c_{l_{max}}$  of plate 1 for different values of  $d$ . It can be observed that the value of lift is high when plate 2 is close to plate 1. But as  $d$  is increased  $c_{l_{max}}$  decreases. For

d<sub>4.5</sub> the value of  $c_{l_{max}}$  remains more or less constant. This shows that the effect of plate 2 on plate 1 is small for d<sub>4.5</sub>.

5. At the same time from figure 10b we can see the variation of  $c_{l_{max}}$  of plate 2 with  $d$ . This plot doesn't follow the trend observed in plate 1.  $c_{l_{max}}$  fluctuates between local minima and maxima as  $d$  changes. This maybe due to constructive or destructive interaction of the wake from plate 1 on the plate2. As  $d$  changes the phase at which the wake makes contact with plate 2 changes. Affecting the value of  $c_{l_{max}}$  of plate 2.

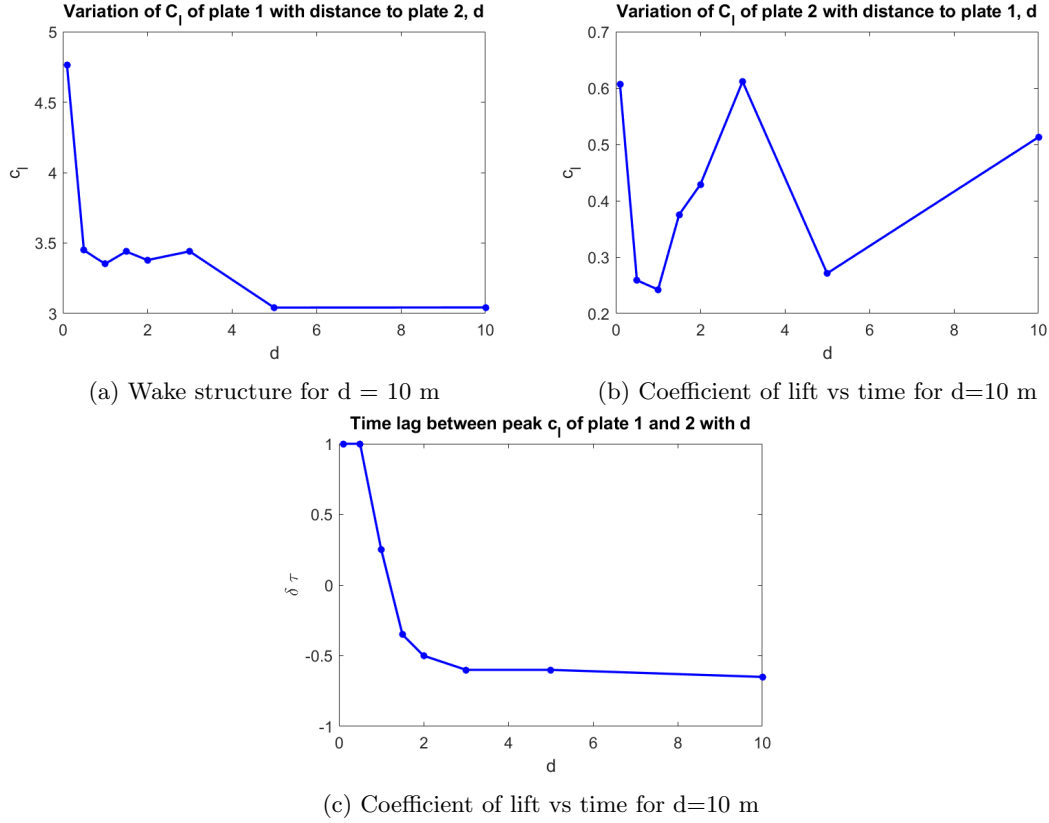


Figure 10

### 5.3 Pitching motion of tandem airfoils at different frequencies

In this subsection we discuss the effect of different reduced frequencies, at a fixed separation. In all the analysis discussed in this subsection  $U_\infty = 5m/s$  and the separation between the flat plates,  $d = 2m$ .



### 5.3.1 $k_2/k_1 = 1$ and $\omega_1 = \omega_2 = 1\text{rad/s}$

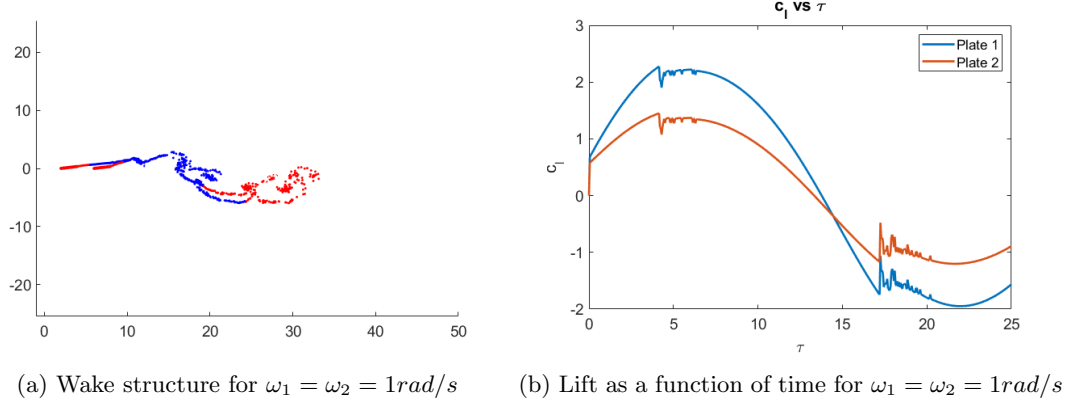


Figure 11

Here both the flat plates undergo sinusoidal motion at the same frequency. The second flat plate has a lower value of maximum lift because of the interaction between the shed vortices from the first plate and the vortices on the second plate.

### 5.3.2 $k_2/k_1 = 1$ and $\omega_1 = \omega_2 = 5\text{rad/s}$

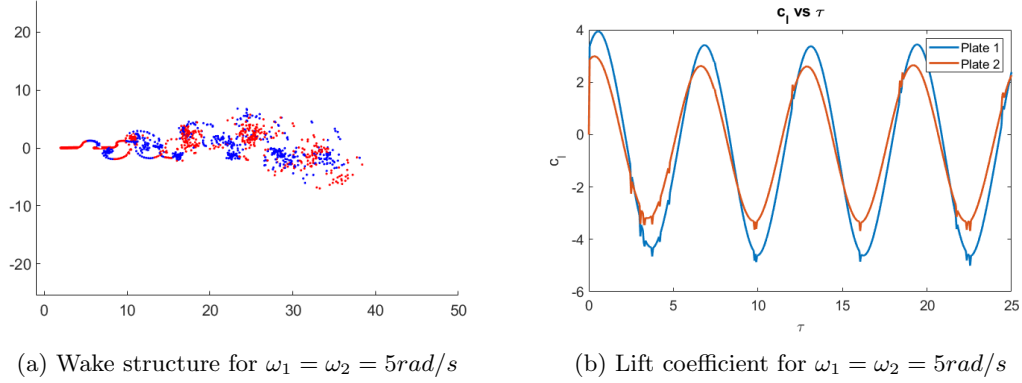
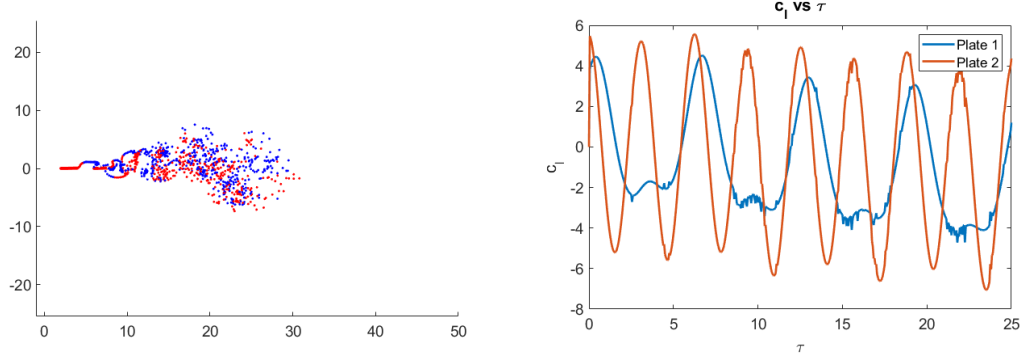


Figure 12

Here again both of the flat plates have the same frequency, but it is  $5\text{rad/s}$ . The wake structure in this case is distinctly different from that of  $\omega = 1\text{rad/s}$ . Hence we can conclude that it's not just the value of  $k_2/k_1$  that determines the wake structure, but rather the individual values of  $k_1$  and  $k_2$  also matter. In both the above cases, we see that the lift curve of the first flat plate leads that of the second flat plate.

### 5.3.3 $k_2/k_1 = 2$ and $\omega_1 = 5\text{rad/s}, \omega_2 = 10\text{rad/s}$

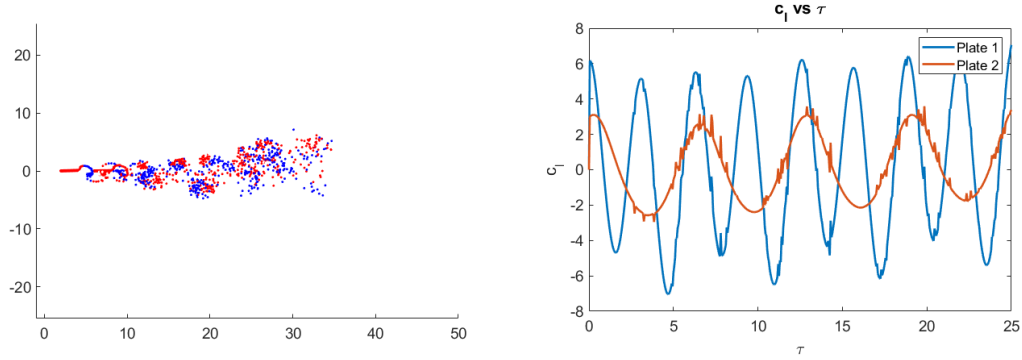


(a) Wake structure for  $\omega_1 = 5\text{rad/s}, \omega_2 = 10\text{rad/s}$  (b) Lift coefficient for  $\omega_1 = 5\text{rad/s}, \omega_2 = 10\text{rad/s}$

Figure 13

The first flat plate is rotated with a frequency of  $5\text{rad/s}$  and the second one is rotated with a frequency of  $10\text{rad/s}$ . The lift in the first flat plate doesn't drop as much as expected, ie, when it approaches its minima a lift restoring mechanism kicks in. However we are not able to explain this lift restoring mechanism in terms of the shed vortices.

### 5.3.4 $k_2/k_1 = 1/2$ and $\omega_1 = 10\text{rad/s}, \omega_2 = 5\text{rad/s}$



(a) Wake structure for  $\omega_1 = 10\text{rad/s}, \omega_2 = 5\text{rad/s}$  (b) Lift coefficient for  $\omega_1 = 10\text{rad/s}, \omega_2 = 5\text{rad/s}$

Figure 14

The second flat plate has a comparatively lower frequency. No lift restoring mechanism as seen in the previous part was observed in this case. The first flat plate has a higher maximum lift, this can be attributed to its relatively higher frequency.

### 5.3.5 $k_2/k_1 = -1$ (phase difference of 180 deg) and $\omega_1 = 5\text{rad/s}, \omega_2 = 5\text{rad/s}$

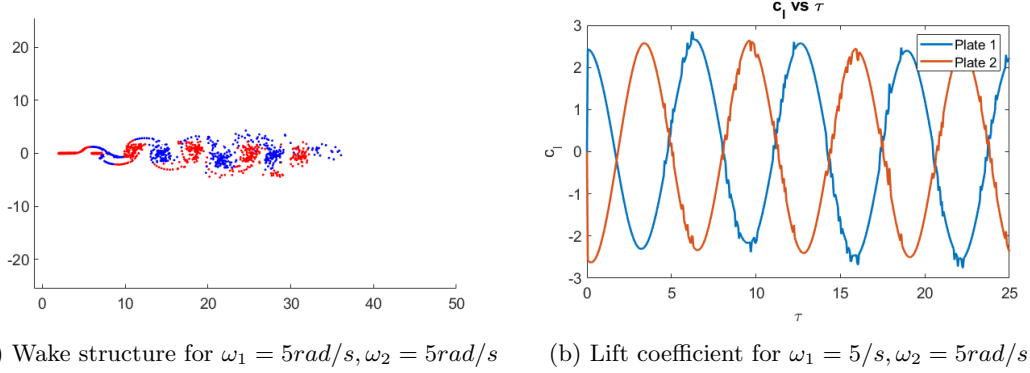


Figure 15

In order to understand the effect of phase difference on the lift, the first flat plate is rotated as  $\alpha_1 = 10^\circ \sin(5t)$  and  $\alpha_2 = -10^\circ \sin(5t)$ . The maximum and minimum value of the lift is same as the case with a phase difference of  $0^\circ$ , However a phase of difference  $\approx 180^\circ$  is observed between the lift curve of both the plates.

## 6 Conclusion

In this project a lumped vortex solver for the unsteady flow past two separated flat plates was developed. The kinematics of the two flat plates were varied to gain insights on the effect of the interaction between the two plates. The lumped vortex method can be used to explore the parameter space and to understand the general trends instead of making use of high fidelity CFD solvers which might take hours if not days to run one single simulation. This makes the lumped vortex method feasible for coupling with an optimizer to find the set of parameters that maximize a given objective function, say the average lift in one cycle.

## References

- [1] Flying fish twist to soar. *Physics world*, 30(8), 2017.
- [2] Joseph Katz and Allen Plotkin. *Low-speed aerodynamics*. Cambridge University Press 2001, 2001.
- [3] Alavaro Martin Sampayo. *Analysis of the effect of gusts on an array of plates with ground effect*. Universidad Carlos III de Madrid, 2014.
- [4] Aziz and Mukherjee R. Vortex interaction and roll-up in unsteady flow past tandem airfoils. *Journal of Applied Fluid Mechanics*, 9(6):3087–3100, 2016.